Numerical and experimental evaluation of lateral torsional buckling of beams at elevated temperatures

P.A.G. Piloto[1], P.M.M. Vila Real[2], J.-M. Franssen[3]
[1]*Mechanical Department, Polytechnic of Bragança, Portugal.*
[2]*Civil Department, University of Aveiro, Portugal.*
[3]*Civil Department, University of Liège, Belgium.*

Abstract

When a beam is bent about its greatest flexural resistance axis it may twist and move laterally, before it reaches its strength limit. Although this problem of lateral torsional buckling of steel beams at room temperature is well known, the same problem at elevated temperature is not.

This paper summarises the results obtained in the scope of a research project entitled "*Lateral buckling of steel I beams under fire conditions*", where a set of 120 experimental and numerical tests were performed on IPE100 beams, submitted to temperatures varying from 20 °C to 600 °C, to validate a new proposal for the buckling resistance moment of a laterally unrestrained beam under fire conditions.

It will be shown that this new proposal is safer than the Eurocode 3 formulas.

1 Introduction

The structural behaviour at elevated temperatures of steel members that are mainly submitted to bending actions has been thoroughly investigated. The structural stability of laterally unrestrained beams has been studied by several authors [1,2,3] at room temperature. Open section members which have low out of plane flexural rigidities and low torsional and warping rigidities are susceptible to enter in this type of failure.

The lateral torsional buckling of steel beams often controls the design situation of many structural members. The influences of residual stresses and

geometric imperfections in the design buckling moment have been studied by Vila Real and Jean-Marc Franssen [4,5,17]. The procedure has been presented and compared with the design formulas of Eurocode 3, Part 1.2 [6]. The theoretical treatment for this type of instability start from the classic elastic solution of a simple supported beam under uniform bending. These pre-standards also make allowances for different support, load and restrained conditions by providing approximations for those effects to elastic buckling.

Building design beams without lateral restrain may be considered as of secondary importance. However, in same situations, such as industrial buildings and plant areas, beams may not have continuous lateral restrain and could be exposed to this situation [12]. At elevated temperatures this behaviour will be affected by the mechanical and thermal properties changes.

A set of 120 full-scale tests based on a reaction frame and on a hydraulic system will be presented for the study of 0.5 to 6.5 meters beam length. A set of three tests was done for each beam length and loaded temperature. The thermal action will be imposed by means of electro-ceramic resistances heated by a power unit of 70 [kVA]. For increasing the thermal efficiency a ceramic fibre mat has been used for better thermal insulation.

2 Case Study

The simple supported beam with fork supports shown in figure 1 has been studied.

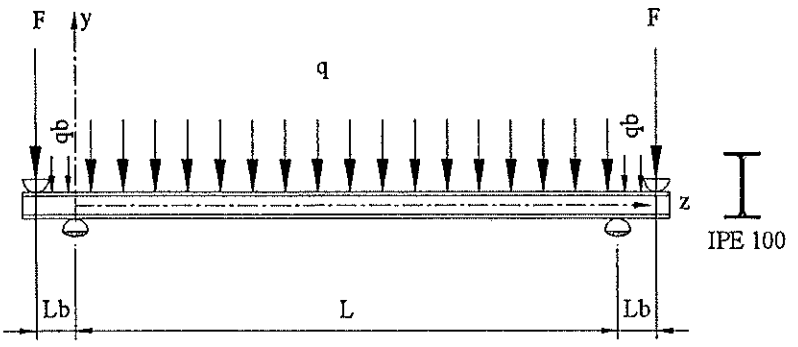

Figure 1: Simple supported beam with tow fork supports.

In this figure, q_b represents the self weight of the beam and q represents the additional distributed load due to the weight of the ceramic mat and electro-ceramic resistances.

Three types of mid span displacements were experimental measured. *DV*, *DLB* and *DLC*, represents the vertical, lateral bottom and lateral top displacement at mid span beam length, as can be seen in figure 2.

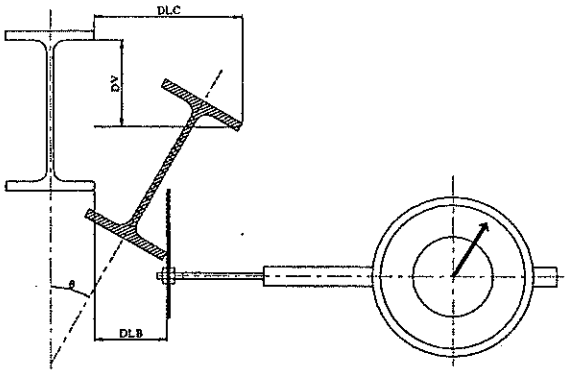

Figure 2: Measured mid span beam displacements.

The thermal action will varies from room temperature up to 200, 300, 400, 500 and 600 [°C]. This action will be applied before the mechanical action, with the longitudinal unrestrained displacement. After temperature stabilisation, the mechanical load process begins, and the relation between load and displacements will varies in accordance to the figure 3.

As long as the loads on the beam remains bellow the critical value, the beam will be stable. However, as the load is increased a critical value is reached when slightly deflected and twisted form of equilibrium becomes possible. The initial plane beam configuration is now unstable, and the lowest load at which this deflected condition occurs is called the beam critical load [16].

The lateral torsional buckling of beams (Figure 3) involves lateral displacement u out of the plane of bending and twist rotations ϕ. In this case, the twist rotations makes the applied moments to have components acting out of the original plane of bending, while the lateral rotations du/dz cause the applied moments to have torque components about the axis of twist through the shear centre.

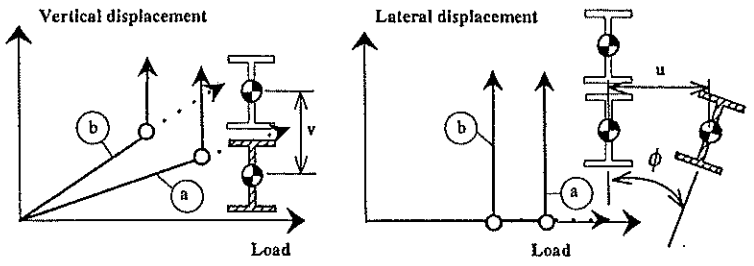

Figure 3: Load versus mid span displacements; a – room temperature, b – elevated temperatures.

The stress strain relationship will be function of material strength and will varies with temperature, according to Eurocode 3 [6].

The geometric imperfections of beam cross section and lateral distortion were measured by means of digital calliper and with the laser beam method. The measured results shown a bigger cross sections dimensions compared to the tabulated values [9].

The reaction frame used to calculate the behaviour of steel IPE100 beams under elevated temperatures is shown in figure 4.

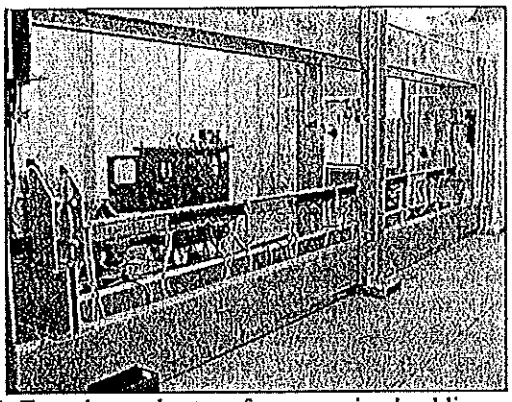

Figure 4: Experimental set-up for measuring buckling resistance at elevated temperature.

The numerical procedure to determine the lateral torsional buckling of beams was based on SAFIR code [10], developed in the University of Liège. A three-dimensional beam element with 15 degrees of freedom and three nodes has been used to calculate the buckling moment resistance of beams loaded as shown in figure 1. All the measured properties and physic characteristics were used in the numerical calculation.

3 Lateral torsional buckling

3.1 Lateral torsional buckling according to the Eurocode 3

The design buckling resistance moment of a laterally unrestrained beam with a class1 or 2 cross section type, in case of fire is given in the Eurocode 3, part 1.2 by

$$M_{b,fi,t,Rd} = \frac{\chi_{LT,fi}}{1.2} W_{pl,y} k_{y,\theta,com} f_y \frac{1}{\gamma_{M,fi}} \tag{1}$$

where

$$\chi_{LT,fi} = \frac{1}{\phi_{LT,\theta,com} + \sqrt{[\phi_{LT,\theta,com}]^2 - [\lambda_{LT,\theta,com}]^2}} \tag{2}$$

with;

$$\phi_{LT,\theta,com} = \frac{1}{2}\left[1 + \alpha(\bar{\lambda}_{LT,\theta,com} - 0.2) + (\bar{\lambda}_{LT,\theta,com})^2\right] \tag{3}$$

and the non dimensional slenderness $\overline{\lambda}_{LT,\theta,com}$, is a function of the maximum temperature in the compression flange, $\theta_{a,com}$

$$\overline{\lambda}_{LT,\theta,com} = \overline{\lambda}_{LT}\sqrt{\frac{k_{y,\theta,com}}{k_{E,\theta,com}}} \tag{4}$$

The remaining factors should be calculated at room temperature, accordingly with the following expressions:

$$\overline{\lambda}_{LT} = \frac{\lambda_{LT}}{\lambda_1} \tag{5}$$

with the slenderness factor λ_{LT} being calculated as function of the critical elastic moment, material elastic modulus and cross section plastic modulus;

$$\lambda_{LT} = \sqrt{\pi^2 \times E \times \frac{W_{pl,y}}{M_{cr}}} \tag{6}$$

and for the slenderness material factor:

$$\lambda_1 = \pi\sqrt{\frac{E}{f_y}} \tag{7}$$

The imperfection parameter α on eqn (3) depends on the type of cross section, being 0.21 for hot rolled sections or 0.49 for welded cross section [7].

3.2 The New Proposal

A new proposal for the lateral buckling resistance, based on numerical calculations has been proposed by Vila Real et al [5,17].

According to this new proposal, and adopting for the lateral torsional buckling the same proposal that Franssen used in 1995 [13] to represent the behaviour of axially-loaded columns when submitted to fire conditions, the design buckling resistance moment of a laterally unrestrained beam can be calculated by

$$M_{b,fi,t,Rd} = \chi_{LT,fi} W_{pl,y} k_{y,\theta,com} f_y \frac{1}{\gamma_{M,fi}} \tag{8}$$

where $\chi_{LT,fi}$, and $\overline{\lambda}_{LT,\theta,com}$ should be calculated as in eqns (2) and (4) and

$$\phi_{LT,\theta,com} = \frac{1}{2}\left[1 + \alpha\overline{\lambda}_{LT,\theta,com} + (\overline{\lambda}_{LT,\theta,com})^2\right] \tag{9}$$

Now the imperfection factor α is a function of a severity factor β [5,17]:

$$\alpha = \beta\varepsilon \tag{10}$$

The severity factor β which should be chosen in order to ensure the appropriate safety level has been taken as 0.65 [5,17], and the material factor calculated by expression

$$\varepsilon = \sqrt{\frac{235}{f_y}} \tag{11}$$

where f_y represents the nominal yield strength of the material.

Comparing eqns (1) and (8) it can be verified that with this new proposal, the empirical constant 1.2 is not used.

Eqns (2) and (9) are exactly the same as those defined at room temperature, except that the threshold limit of 0.2 for $\overline{\lambda}_{LT}$ does not appear in eqn (9). This fact changes the shape of the buckling curve, beginning at $\chi_{LT} = 1.0$ for $\overline{\lambda}_{LT}$ but decreasing even for very low slenderness, instead of having a horizontal plateau up to $\overline{\lambda}_{LT} = 0.4$.

The lateral-torsional buckling curve now depends on the steel grade due to the parameter ε that appears in the imperfection factor as it can be seen in figure 5.

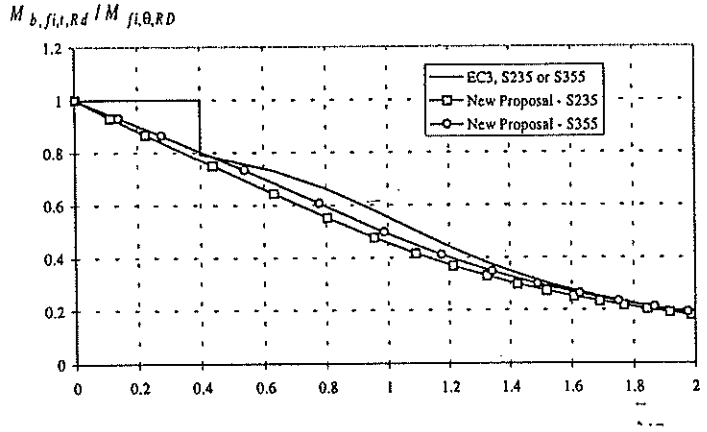

Figure 5: Comparisons between beam design buckling curve of Eurocode 3 and the new proposal.

4 Experimental evaluation

A multifunction reaction structure (figure 4) was used to test the beams at elevated temperatures and apply the mechanical loads. The loads were applied by means of two hydraulic jacks with 60 [ton] each and the beams were heated using electric ceramic mats.

It was used 500 meters of IPE 100 profile, given 120 beams with lengths varying from 0.5 to 6.5 meters.

The initial conditions of the steel beams were measured, specially, the residual stresses, the geometric imperfections and the cross section geometry was dimensionally controlled.

4.1 Residual stresses

The magnitude and geometric distribution of the residual stresses may vary with the geometry of the cross section and with the straightening and cooling processes. The residual stresses were measured in four points as it is shown in figure 6. The measurements were based on the drill hole method [14] and the mean values obtained are shown in figure 6.

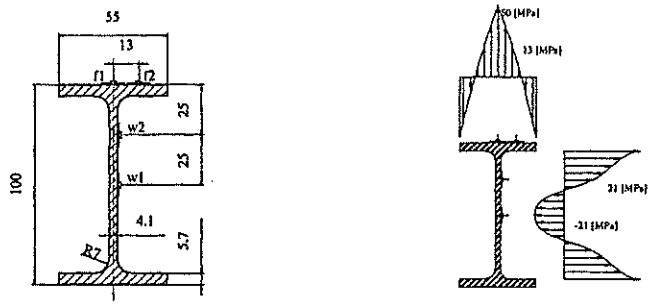

a) b)

Figure 6: a) Residual stresses measurement points. b) Distribution of the measured residual stresses.

4.2 Geometric Imperfections

Two types of geometric imperfections were measured. One related to the cross section dimensions, measured by digital callipers and the second one related to the longitudinal lateral distance relatively to a imaginary straight line, measured by a laser beam method, the Helium Neon 30 mW – classe III b. All measured imperfection beams have been approximated by the following expression:

$$u(z) = a.Sin\left(\frac{\pi \times z}{L}\right) \tag{12}$$

where a is the measured maximum amplitude of the geometric beam imperfection.

The cross section geometry imperfections were also measured and used in the numerical calculation.

A set of 31 profiles from the 46 originals was used to compare the cross section strength related to geometric data. The calculated plastic modulus exceeds the foreseen values.

4.3 Material strength characterisation

A set of 20 specimens was tested on the 4485 Instron universal machine with 200 [kN] maximum capacity. The specimens were machined from the flanges and web parts from the IPE100 beams, and follow the Portuguese

standard NP EN10002-1 [15], for yield strength and elastic modulus characterisation.

4.4 Thermal action

Two different types of electro ceramic mat resistance's with 1220 x 45 and 610 x 85 [mm], with a maximum electric power of 2.7 [kW] each, were used to heat the beams. This material is capable to support temperatures up to 1050 [°C], although our experiments were done only up to 600 [°C] and with a heat rate of 800 [°C/h].

4.5 Mechanical actions

The mechanical load was applied after temperature stabilisation. The concentrated load F (see figure 1) was incremented by amounts of 2000 [N] till a certain value in witch a increase in displacement value didn't correspond to a load increase. This value will be considered as the collapse load, as can be seen in next figure 7.

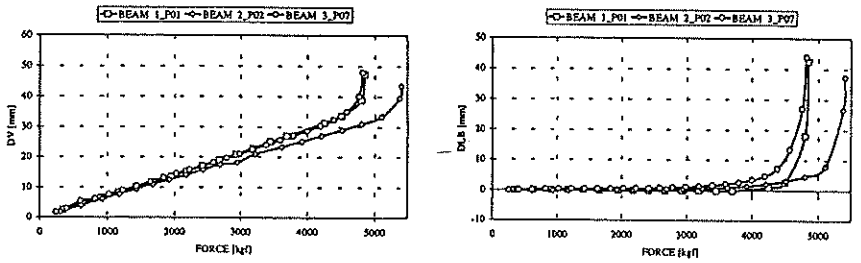

Beam at room temperature

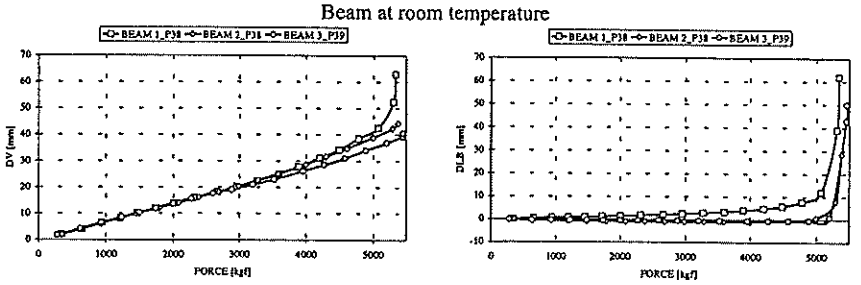

Beam at temperature 200 [°C]

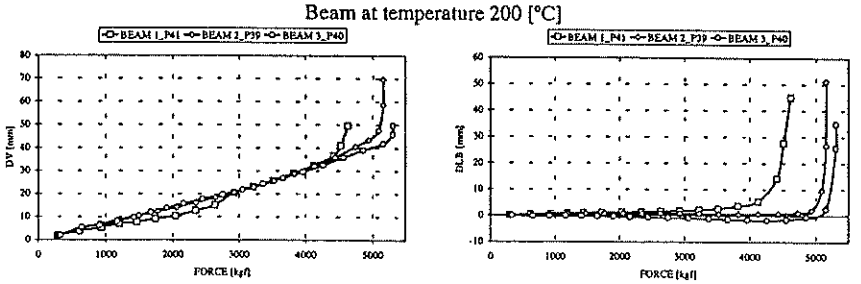

Beam at temperature 300 [°C]

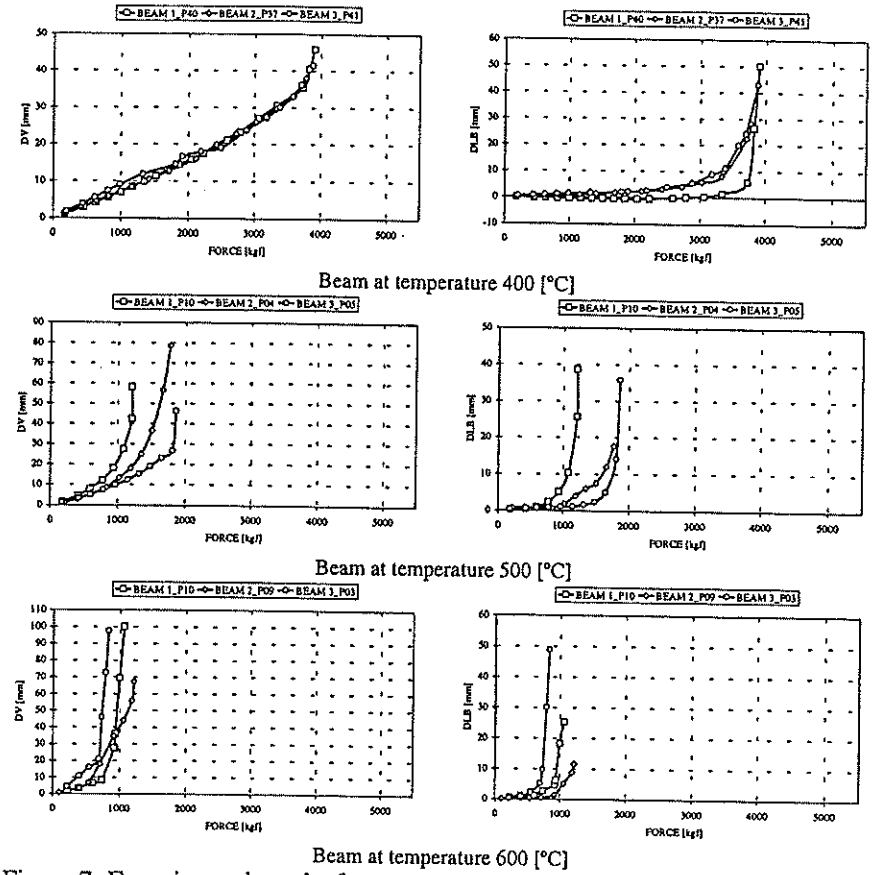

Figure 7: Experimental results from room temperature up to 600 [°C] on a 3.5 [m] span beam.

In all graphic representation, *DV* represents the vertical displacement and *DLB* represents the bottom lateral displacement. The lateral top displacement *DLC* was also recorded, but omitted in this figure. Figure 7 shows that the critical load decrease as the temperature increase.

4.6 Lateral buckling design curves

The experimental results for all tested temperatures were plotted in the same chart presented in figure 8. The curve for the new proposal is safer than the eurocode 3 curve.

5 Numerical evaluation

A set of 120 numerical calculations were made to calculate the beam design buckling moment at elevated temperatures. A non linear material and geometrical code [10,11], based on two types of finite elements, make possible

the lateral torsional buckling study of the IPE100 beams. Bi-dimensional plane linear elements were used to describe the temperature result from the thermal action [8]. The warping function and the torsion resistance have been calculated for each temperature level, considering the beams geometric imperfection, the residual stresses and the material property values, according to the experimental measuring and their temperature dependence according to the Eurocode 3.

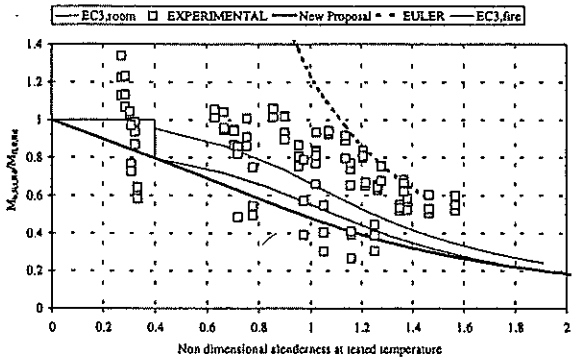

Figure 8: Beam design curves at elevated temperatures. Experimental results.

The critical moment obtained by numerical simulation were used to plot the chat of figure 9. These numerical results show once again that the new proposal is safer than the Eurocode 3 curve.

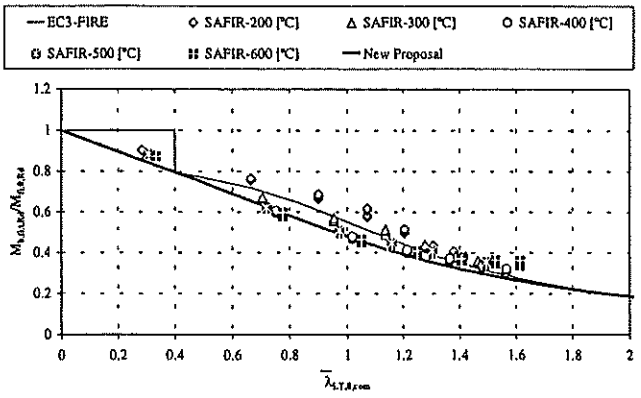

Figure 9: Beam design curves at elevated temperatures. Numerical results.

6 Experimental and numerical comparison

Both experimental and numerical results have been compared with the simply formulas from Eurocode and with the new proposal. Each point in figure 10 represents an experimental test.

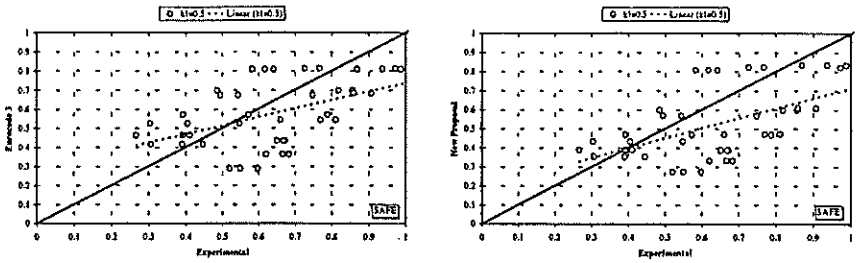

Figure 10: Experimental behaviour, for higher temperatures (above 400[°C]).

The same type of result can be presented to the numerical simulations as shown in figure 11. As in the previous figure, the pending from global results, are close to the ideal continuous line, for higher temperatures.

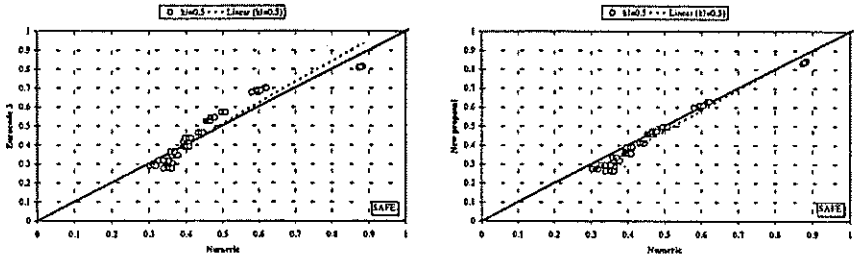

Figure 11: Numerical behaviour, for higher temperatures (above 400[°C]).

The number of unsafe points is smaller in the case of the new proposal. This simply new formula seams to give safer results.

7 Conclusions

The physical fact that elasticity modulus decreases faster than the yield strength when the temperature increases, plus the fact that the stress-strain relationship at elevated temperature is not the same as at room temperature, produce a modification of the lateral-torsional buckling curve at elevated temperature. The horizontal plateau valid at 20 °C up to a non-dimensional slenderness of 0.4 may vanishes in the case of elevated temperatures as presented in the new proposal.

The simple models based on the lateral-torsional buckling curve that is valid at room temperature lead to a safety level that depends on the slenderness of the beam, being unsafe for intermediate length beams. It has been shown that the new proposal for lateral torsional buckling, based on the proposal suggested earlier [13] for axially-loaded hot-rolled H-sections submitted to fire is safer that the Eurocode 3 formulas.

Acknowledgements

This work is a result of the Portuguese Project of R&D that was financed by the Portuguese Foundation for Science and Technology (MCT/FCT) with the participation of the University of Aveiro and the Polytechnic of Bragança (Portugal).

Special thanks to Prof. Mario Vaz (University of Porto) are due.

The authors acknowledge the contribution of the enterprise J. Soares Correia, by the 500 [m] of IPE 100 beams that were tested in Bragança.

References

[1] Trahair N.S.; " Flexural – Torsional Buckling of structures"; E&FN SPON – Chapman & Hall; London; 1993.

[2] Timoshenko P.S.; Gere J.M.; "Theory of elastic stability"; McGraw Hill International editions – Mechanical Engineering series; 2nd edition; 1963.

[3] Papangelis, J.P.; Trahair, N.S.; Hancock, G.J.; "Elastic flexural-torsional buckling of structures by computer"; Journal of Computers and Structures 68 (1998); Pergamon Press; 125-137.

[4] Vila Real, P.M.M.; Franssen, Jean - Marc; "Lateral buckling of steel I beams at room temperature - Comparison between the EUROCODE 3 and the SAFIR code considering or not the residual stresses", internal report No. 99/01 , Institute of Civil Engineering – Service Ponts et Charpents – of the University of Liege. 1998.

[5] Vila Real, P.M.M.; Franssen, Jean - Marc; "Lateral buckling of steel I beams under fire conditions - Comparison between the EUROCODE 3 and the SAFIR code", internal report No. 99/02 , Institute of Civil Engineering – Service Ponts et Charpents – of the University of Liege. 1999.

[6] CEN ENV 1993-1-2; "Eurocode 3 – Design of steel structures – Part 1-2: General Rules – Structural fire design";1995.

[7] CEN ENV 1993-1-1; "Eurocode 3, Design of Steel Structures – Part 1-1: General rules and rules for buildings"; April 1992.

[8] CEN ENV 1991-2-2; "Eurocode 1, Basis of design and actions on structures – Part 2-2: Actions on structures – Actions on structures exposed to fire"; 1995.

[9] Tabulated data; Arbed research centre; Luxembourg; 1987.

[10] Franssen, Jean-Marc; "Safir users manual"; ver 1.3; 1995.

[11] Franssen, Jean-Marc; "Contribuition à la modelisation des incendes dans les batiments et leur effects sur les structures"; thése présentée en vue de l'obtention du grade d'agrégré de l'enseignement Supérieurs; Université de Liége; Année academique 1997/98.

[12] Reis, António; Camotim Dinar; "Estabilidade Estrutural"; McGraw Hill; Outubro 2000.

[13] Franssen, Jean-Marc; Schleich, Jean Baptist; Cajot, Louis-Guy; " A simple model for fire resistance of axially-loaded members according to Eurocode 3"; Journal Construct. Steel Research, Vol. 35; pp. 49-69; 1995.

[14] Hoffman Karl; " An introduction to measurements using strain gages"; HBM publisher; Germany; 1989.

[15] NP EN 10 002-1; CT12, Materiais metálicos:; "Ensaio de tracção. Parte 1: Método de ensaio"; Insituto Português da Qualidade; 1990.

[16] Singer, J.; Arbocz, J.; Weller, T.; "Buckling Experiments- Experimental methods in Buckling of Thin Walled structures"; Volume 1; John Wiley & Sons; England; 1998.

[17] VILA REAL, P. M. M.; FRANSSEN, J. M. – *"Numerical Modelling of Lateral Buckling of Steel I Beams Under Fire Conditions – Comparison with Eurocode 3"*, accepted for publication on Vol. 11, No. 2 (May 2001), Journal of Fire Protection Engineering, The International Journal of the Society of Fire Protection Engineers, USA.